

# Theoretical study of a surface electrode reaction preceded by a homogeneous chemical reaction under conditions of square-wave voltammetry

Rubin Gulaboski <sup>a,\*</sup>, Valentin Mirčeski <sup>b</sup>, Milivoj Lovrić <sup>c</sup>, Ivan Bogeski <sup>d</sup>

<sup>a</sup> *Faculdade de Ciências, Universidade do Porto, Rua do Campo Alegre 687, Porto, Portugal*

<sup>b</sup> *Department of Chemistry, Faculty of Natural Sciences and Mathematics, “Sts. Kiril i Metodij” University, Skopje, Macedonia*

<sup>c</sup> *Ruder Bosković Institute, Zagreb, Croatia*

<sup>d</sup> *Department of Physiology, University of Saarland, Homburg, Germany*

Received 23 February 2005; received in revised form 10 March 2005; accepted 10 March 2005

Available online 2 April 2005

## Abstract

A theoretical model of a surface electrode reaction coupled with a preceding chemical reaction (surface CE electrode mechanism) is theoretically studied under conditions of square-wave voltammetry. The position and the shape of the theoretical voltammograms are function of the redox kinetic parameter  $\lambda = \frac{k_s}{f}$  where  $k_s$  is the standard electron exchange rate constant and  $f$  is the frequency of the potential modulation, chemical kinetic parameter  $z = \frac{k_f + k_b}{f}$ , where  $k_f$  and  $k_b$  are the forward and backward rate constants of the preceding chemical reaction, respectively, and the equilibrium constant of the chemical reaction  $K$ . The influence of all these parameters to the theoretical square-wave voltammograms is investigated in detail. A theoretical methodology for estimation of the kinetic and thermodynamic parameters of the electrode mechanism is proposed.

© 2005 Elsevier B.V. All rights reserved.

**Keywords:** Surface CE reaction; Square-wave voltammetry; Quasireversible maximum; Split SW voltammograms; Mathematical modelling

## 1. Introduction

Electrode reactions coupled with homogeneous or heterogeneous chemical reactions have been intensively studied with various voltammetric techniques in the past few decades [1–26]. A large number of theoretical and experimental studies have been devoted to elucidate the complex voltammetric behaviour of such systems and a variety of methodologies for determination of the kinetics and/or thermodynamics of the chemical reactions have been developed [2–26]. Among voltammetric techniques, cyclic voltammetry (CV) is the most popular. This is due to its feasibilities for relatively easy

consideration of diverse reaction mechanisms [14,24–26]. In the last two decades, however, square-wave voltammetry (SWV) replaces considerably CV in analytically oriented studies or studies concerned with the mechanism of the electrode reaction [2–23,27–35]. The SWV is capable to discriminate the charging current as well as to provide an insight into both half-electrode reactions, making this technique particularly suitable for studying the electrode mechanism [2–23,27–35]. Several electrode mechanisms involving chemical reactions under semi-infinite diffusion mass transfer in SWV have been studied by Osteryoung and O’Dea [2,4] and others [16–20,22,23]. Beside the diffusion controlled electrode reactions, significant attention has also been paid to the diffusionless electrode reactions, e.g., the surface electrode reactions [3,13,14,21,24–26,28–35]. It has been

\* Corresponding author. Fax: +351 226 082 959.

E-mail address: [rubingulaboski@excite.com](mailto:rubingulaboski@excite.com) (R. Gulaboski).

shown that the voltammetric responses of a surface electrode reaction possess unique features such as a “quasi-reversible maximum” [13,14,28–35] and “split SW peaks” [13,14,31,34], which both can be utilized for the determination of the kinetics of the electrode reaction. Moreover, in recent papers, the properties of a surface catalytic electrode reaction were elaborated in detail, establishing criteria for measuring the kinetics of the catalytic reaction [13,14].

In this paper, we are presenting a theoretical model for a surface electrode reaction preceded by a homogeneous chemical reaction (surface CE mechanism) under conditions of SWV. Experimental examples of such electrode mechanism can be found in many studies based on the so called “ligand-induced adsorption of complexes” [see for example Review papers 36a and b]. Moreover, the surface CE reactions is a reaction pathway for numerous electroactive proteins immobilized on the electrode surface studied by means of “protein-film voltammetry” developed by Armstrong et al. [37–40]. To the best of our knowledge, the surface CE mechanism has not yet been considered theoretically under conditions of square-wave voltammetry.

## 2. Mathematical model

An electrode reaction preceded by a chemical reaction is considered:



All participants in the electrode mechanism are irreversibly immobilized on the electrode surface. During the voltammetric experiment the mass transport of all species can be neglected.  $k_f$  ( $\text{s}^{-1}$ ) and  $k_b$  ( $\text{s}^{-1}$ ) are the first order rate constants of the forward and backward chemical reaction, respectively. In practice, the forward chemical reaction is of a pseudo-first order, undergoing as  $X(\text{aq}) + A(\text{ads}) \rightarrow B(\text{ads})$ , characterized by the second order rate constant  $k'$  ( $\text{mol}^{-1} \text{cm}^3 \text{s}^{-1}$ ). Here X is a certain reactant present in the solution in a large excess, the concentration of which is constant during the voltammetric experiment. Hence,  $k_f$  is a pseudo-first order rate constant defined as  $k_f = k'_f c(X)$ .

The electrode mechanism (I) is mathematically represented by the following model:

$$\frac{d\Gamma(\text{A})}{dt} = k_b\Gamma(\text{B}) - k_f\Gamma(\text{A}), \quad (1)$$

$$\frac{d\Gamma(\text{B})}{dt} = -\frac{I}{nFS} - k_b\Gamma(\text{B}) + k_f\Gamma(\text{A}) \quad (2)$$

$$\frac{d\Gamma(\text{C})}{dt} = \frac{I}{nFS} \quad (3)$$

$$t = 0:$$

$$\Gamma(\text{A}) = \Gamma_0(\text{A}); \quad \Gamma(\text{B}) = K\Gamma_0(\text{A}); \quad \Gamma(\text{C}) = 0; \\ \Gamma_0(\text{A}) + \Gamma_0(\text{B}) = \Gamma_0; \quad K = k_f/k_b, \quad (\text{a})$$

$$t > 0:$$

$$\Gamma(\text{A}) + \Gamma(\text{B}) + \Gamma(\text{C}) = \Gamma_0 \quad (\text{b})$$

Here,  $\Gamma_0(\text{A})$  and  $\Gamma_0(\text{B})$ , are the initial surface concentrations of the species A and B, respectively, while  $\Gamma_0$  is the total surface concentration of all species.  $\Gamma$  is the surface concentration of particular specie that is a function of time  $t$ .  $K$  is the equilibrium constant of the chemical reaction,  $S$  is the electrode surface area and the other symbols have their usual meaning. The solutions of Eqs. (1)–(3) were obtained by means of Laplace transformations. The solutions for the surface concentrations of the electroactive species B and C, in a form of integral equations read

$$\Gamma(\text{B}) = \frac{K(\Gamma_0 - \int_0^t \frac{I(\tau)}{nFS} d\tau) + \varepsilon^{-1} \int_0^t \frac{I(\tau)}{nFS} \exp(-\varepsilon\tau) d\tau}{1 + K} \quad (4)$$

$$\Gamma(\text{C}) = \int_0^t \frac{I(\tau)}{nFS} d\tau \quad (5)$$

In Eq. (4), the parameter  $\varepsilon$  is defined as  $\varepsilon = k_f + k_b$ . In addition, at the electrode surface the following condition holds:

$$\frac{I(\tau)}{nFS} = k_s \exp(-\alpha\phi) [\Gamma(\text{B}) - \exp(\phi)\Gamma(\text{C})] \quad (6)$$

where  $k_s$  ( $\text{s}^{-1}$ ) is the heterogeneous electron exchange rate constant corresponding to the standard redox potential  $E_{\text{B/C}}^0$  of the electrode reaction (II),  $\alpha$  is the cathodic electron transfer coefficient, and  $\phi = \frac{nE}{RT}(E - E_{\text{B/C}}^0)$  is the dimensionless relative electrode potential. Substituting Eqs. (4) and (5) into Eq. (6) yields

$$\frac{I(\tau)}{nFS} = k_s \exp(-\alpha\phi) \\ \times \left[ \frac{K(\Gamma_0 - \int_0^t \frac{I(\tau)}{nFS} d\tau) + \varepsilon^{-1} \int_0^t \frac{I(\tau)}{nFS} \exp(-\varepsilon\tau) d\tau}{1 + K} \right. \\ \left. - \exp(\phi) \int_0^t \frac{I(\tau)}{nFS} d\tau \right]. \quad (7)$$

Integral Eq. (7) is a general mathematical solution of the surface CE electrode mechanism. Numerical solution of the Eq. (7) adopted for SWV was obtained according to the method of Nicholson and Olmstead [41]. For numerical solution the time increment  $d$  was defined as  $d = 1/(50f)$ , where  $f$  is the frequency of the potential modulation. It means that each SW half-period  $\tau/2$  was divided into 25 increments. The numerical solution reads:

$$\Psi_m = \left[ \frac{K\lambda(1+K)^{-1} \exp(-\alpha\phi) (1 - (50)^{-1} \sum_{j=1}^{m-1} \Psi_j) - \lambda(50)^{-1} \exp((1-\alpha)\phi) \sum_{j=1}^{m-1} \Psi_j + z^{-1} \lambda(1+K)^{-1} \exp(-\alpha\phi) \sum_{j=1}^{m-1} \Psi_j S_{m-j+1}}{K\lambda(1+K)^{-1} \exp(-\alpha\phi) (50)^{-1} + \lambda(50)^{-1} \exp((1-\alpha)\phi) - z^{-1} \lambda(1+K)^{-1} S_1 \exp(-\alpha\phi)} \right] \quad (8)$$

Here,  $\lambda$  is the dimensionless redox kinetic parameter,  $\lambda = \frac{k_s}{f}$ ,  $z$  is the dimensionless chemical kinetic parameter,  $z = \frac{e}{f}$ , and  $S_m$  is the numerical integration factor  $S_m = \exp(\frac{-mz}{50}) - \exp(\frac{z(-m+1)}{50})$ .  $\Psi_m$  is the dimensionless current defined as  $\Psi_m = \frac{I_m}{nFSfT_0}$ .

### 3. Results and discussion

#### 3.1. Slow electron transfer

Theoretical net SW voltammograms are bell-shaped curves characterized by peak potential  $E_p$ , peak current

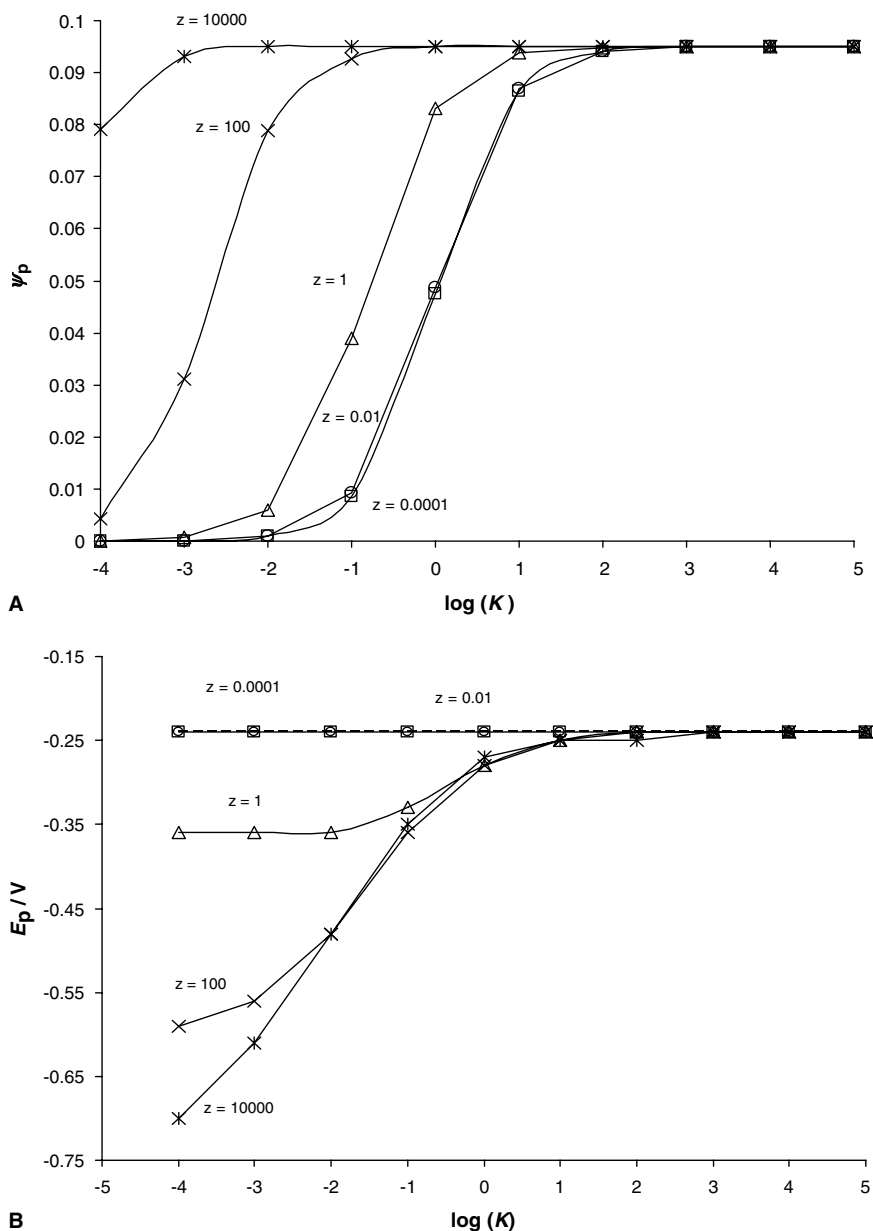


Fig. 1. Slow electron transfer: Theoretical dependences of the dimensionless net peak currents  $\Psi_p$  (A) and the peak potentials  $E_p$  (B) on the logarithm of the equilibrium constant  $\log(K)$  estimated for different values of chemical parameter  $z$ . The other parameters were:  $\lambda = 0.01$ , SW amplitude  $E_{sw} = 50$  mV,  $\alpha = 0.5$ ,  $n = 1$ , and  $T = 298$  K.

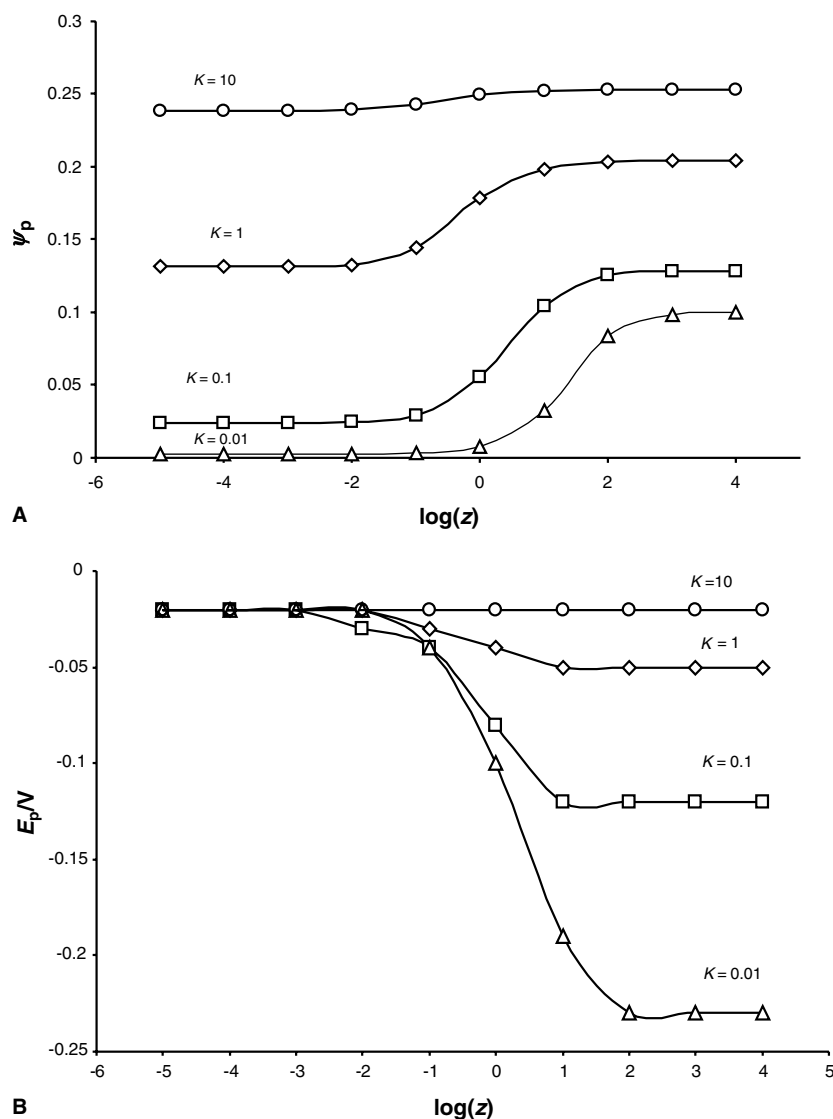


Fig. 2. *Slow electron transfer*: Theoretical dependences of the dimensionless net peak currents  $\Psi_p$  (A) and the peak potentials  $E_p$  (B) on the logarithm of the chemical parameter  $\log(z)$  simulated for different values of  $K$ . The value of  $\lambda$  was 0.126. The other parameters were the same as in the caption of Fig. 1.

$\Psi_p$ , and half-peak width  $\Delta E_{p/2}$ . These parameters of the response are mainly dependent on the potential modulation parameters (frequency- $f$ , amplitude- $E_{sw}$ ), as well as of the redox kinetic parameter  $\lambda$  ( $\lambda = \frac{k_s}{f}$ ), the chemical kinetic parameter  $z$  ( $z = \frac{\epsilon}{f} = \frac{k_f + k_b}{f}$ ), and the equilibrium constant  $K$ .

The effect of the preceding reaction is represented by the chemical kinetic parameter  $z$  and the thermodynamic parameter  $K$ . In general, the overall dependencies of  $\Psi_p$  vs.  $\log(K)$  can be approximated with a sigmoidal function. Regardless of the value of the chemical kinetic parameter, for  $\log(K) \geq 2$ ,  $\Psi_p$  is a constant (Fig. 1A). This is the case when the initial concentration of B is much larger than A due to the strong shift of the chemical equilibrium (I) towards the right-hand side. Under these conditions, the response of the surface CE mecha-

nism is equivalent to the simple surface electrode reaction [3,34]. For  $\log(K) < 2$ , the peak current depends strongly on  $K$  (Fig. 1A). The lower plateau of the curves in Fig. 1A corresponds to the so-called “frozen equilibrium”, i.e., when the preceding chemical reaction produces a minute amount of the electroactive reactant.

For low values of  $z$  (i.e.,  $\log(z) \leq -2$ ), when the chemical reaction is very slow, the peak position is unaffected by the equilibrium constant (see Fig. 1B). For  $\log(z) \geq 0$ , the peak potential shifts linearly to more positive values by increasing  $\log(K)$  over the interval  $-2 < \log(K) < 1$  (Fig. 1B).

Fig. 2A shows the effect of the chemical kinetic parameter on the net SW peak current for several values of the equilibrium constant. The linear part of the curves corresponds to the situation when the peak current is

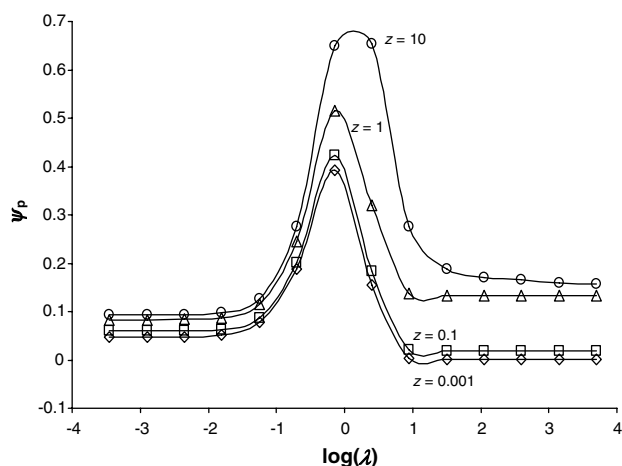


Fig. 3. *Slow electron transfer*: Theoretical dependences of the dimensionless peak currents  $\Psi_p$  on the logarithm of the kinetic parameter  $\log(\lambda)$  simulated for different values of  $z$  and  $K=1$ . The other parameters were the same as in the caption of Fig. 1.

controlled by the kinetics of the preceding chemical reaction. As the kinetics of the preceding chemical reaction increases, the surface concentration of the electro-

active reactant B also enhances in the course of the voltammetric experiment causing a corresponding enlargement of the peak current. When the preceding chemical reaction is very fast, i.e.,  $\log(z) \geq 3$ , the peak current is independent of  $z$ , since the equilibrium of the preceding reaction is maintained all throughout the voltammetric experiment (Fig. 2A).

Fig. 2B shows the variation of the peak potential with the chemical kinetic parameter. Over the interval  $-1 \leq \log(z) \leq 2$ , for  $\log(K) > -2$ , the peak potential depends linearly on  $\log(z)$ , with a slope equal to  $2.303 \frac{RT}{nF} \log\left(\frac{K}{1+K}\right)$ . Therefore, the linear dependence of the peak potential on the chemical kinetic parameter is of particular importance since it provides both kinetic and thermodynamic information on the preceding chemical reaction. These results agree qualitatively with chronoamperometric measurements of the dehydration kinetics of some carbonyl compounds [36].

One of the most intriguing features of the SW voltammetric response of a surface electrode reactions is the “quasireversible maximum” [13,14,28–33,35], which is manifested as a parabolic dependence of the dimensionless net peak current on the logarithm of the redox

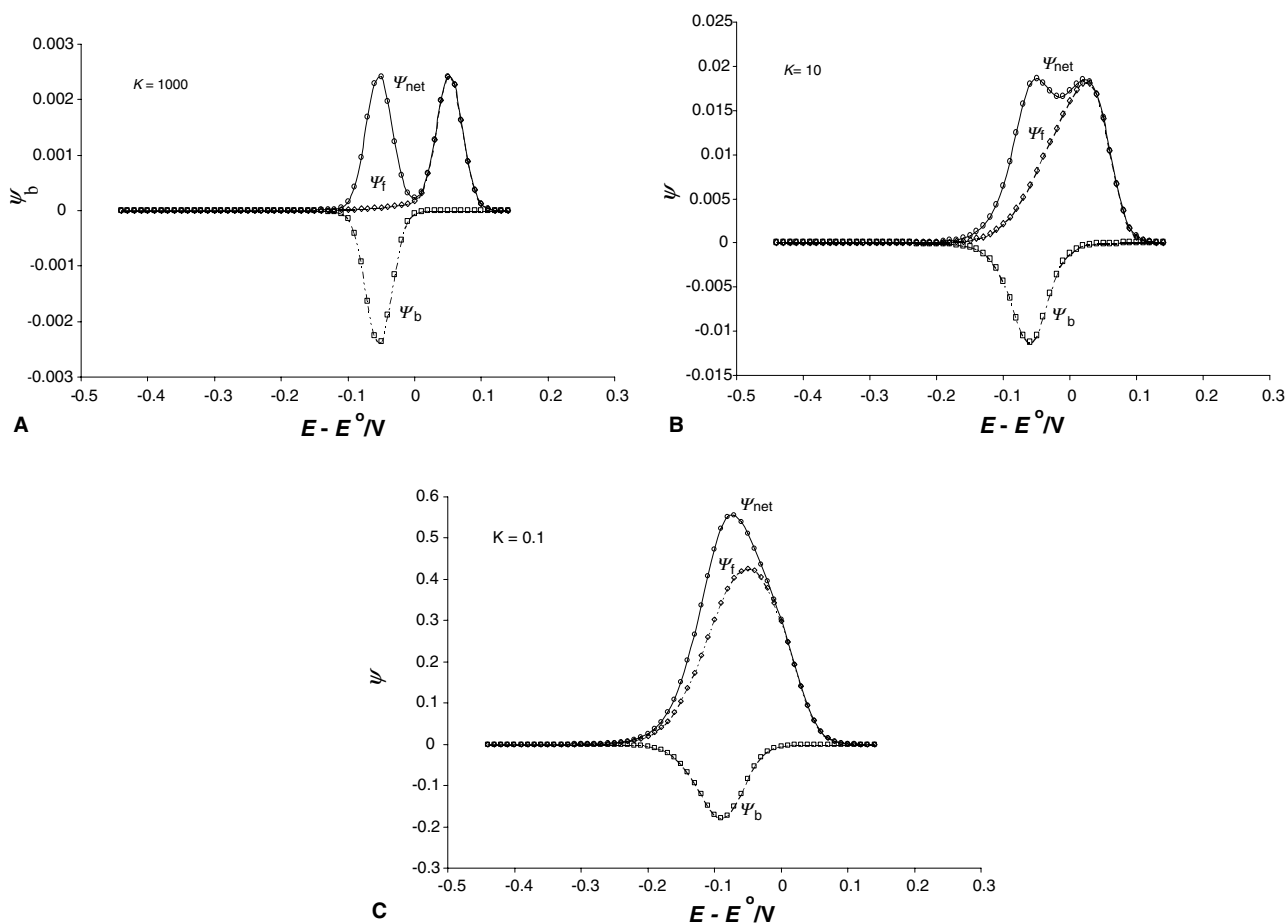


Fig. 4. *Fast electron transfer*: Simulated square-wave voltammograms showing the effect of the equilibrium constant  $K$  to the shape of the voltammetric responses.  $E_{sw} = 60$  mV,  $\lambda = 10$ ,  $z = 10$ .  $\Psi_{net}$ ,  $\Psi_f$  and  $\Psi_b$  stand for the net, forward and backward components of the square-wave voltammograms, respectively. The other parameters were the same as in the caption of Fig. 1.

kinetic parameter  $\lambda$ . The origin and properties of the quasireversible maximum has been elaborated in detail [28,29,35]. Its importance stems from the fact that it can be exploited for estimation of the electron transfer kinetics [13,14,28–33,35]. Shown in Fig. 3 are the dependences of  $\Psi_p$  on  $\log(\lambda)$  simulated for various values of the chemical kinetic parameter  $z$  and equilibrium constant  $K=1$ . In all cases a well-developed parabolic dependence between  $\Psi_p$  and  $\log(\lambda)$  exists. Obviously, the chemical parameter  $z$  does not influence the position

of the quasireversible maximum. This is a very important finding since it shows that the position of the quasireversible maximum does not depend on the kinetics of the preceding chemical reaction. It is also worth noting that the thermodynamics of the preceding chemical reaction, portrayed through  $K$ , also does not influence the position of the quasireversible maximum (data not shown). Consequently, the feature of quasireversible maximum can be solely exploited for determination of the electron exchange standard rate constant ( $k_s$ ) for a

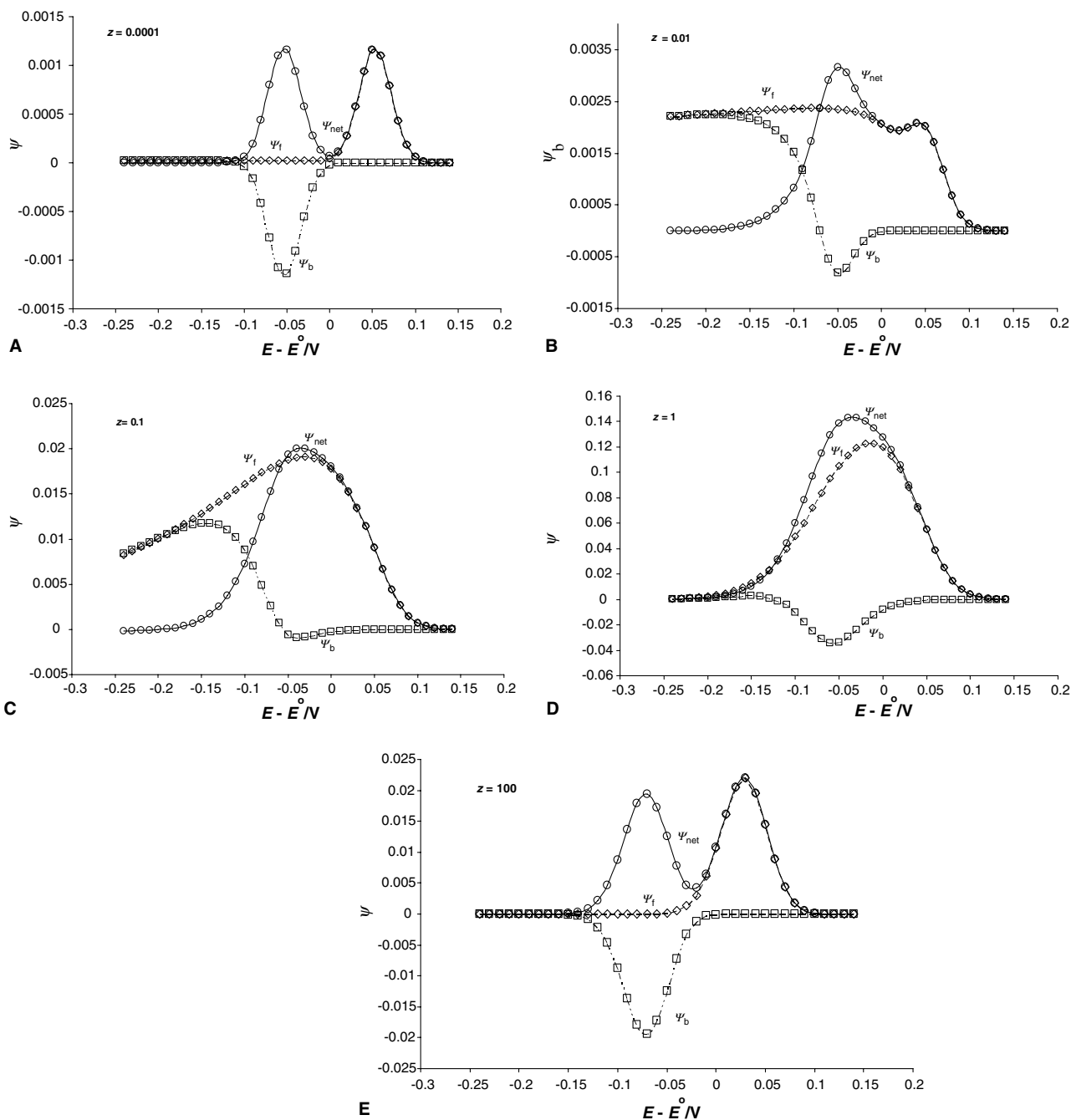


Fig. 5. Fast electron transfer: Simulated square-wave voltammograms showing the effect of the chemical parameter  $z$  to the shape of the voltammetric responses.  $E_{sw} = 60$  mV,  $\lambda = 10$ ,  $K = 1$ . The other parameters were the same as in the caption of Fig. 1.

surface CE mechanism following the procedure described in [13,28–33,35].

### 3.2. Fast electron transfer

The most remarkable feature of the fast surface electrode reaction is the *splitting of the net SW peak* [31,34]. By increasing the amplitude, or decreasing the frequency of the potential modulation, the single net SW response of a surface electrode reaction splits in two peaks [13,31,34]. The origin and properties of the splitting have been thoroughly examined, demonstrating that this phenomenon can be exploited for complete kinetic and thermodynamic characterization of the surface electrode reaction through a simple procedure [34].

For the surface CE mechanism, however, the potential separation between the split SW peaks is affected by the equilibrium constant  $K$  and the chemical kinetic parameter  $z$ . Shown in Figs. 4 and 5 is the influence of  $K$  and  $z$ , respectively, to the shape of the voltammetric response under conditions of splitting. The equilibrium constant  $K$  affects the splitting only if  $\log(z) \geq 1$ . For  $\log(K) \geq 2$ , the split SW voltammograms of the surface CE reaction are identical with those of a simple surface electrode reaction (Fig. 4A). Within the interval  $-1 < \log(K) < 2$ , the potential separation between the split SW peaks decreases by decreasing of  $K$ , and the splitting finally vanishes for  $\log(K) \leq -1$ .

Interesting phenomena related with the splitting have been observed upon increasing of the chemical kinetic parameter  $z$ , varied over the interval of  $-3 \leq \log(z) \leq 2$  (Fig. 5). As the chemical kinetic parameter  $z$  controls the production of the electroactive reactant B during the voltammetric experiment, an increase of  $z$  causes an increase of  $I(B)$ , thus causing an enhancement of the forward component of the SW response (Fig. 5A–C). After reduction of the initial amount of B, the chemical reaction supplies the system with additional amount of B, causing a lifting of the descending branch of the forward component (compare Figs. 5B and C). Further enlargement of the chemical kinetic parameter transforms both the forward and backward components into sigmoidal curves (Fig. 5C), which is similar to the surface catalytic mechanism [13,14]. This re-supply of the electrode surface with the electroactive material requires additional energy for its electrochemical transformation, which is manifested as a shift of the forward component towards more negative potentials by increasing of  $z$ . This is the reason for the decreasing of the potential separation between the split net SW peaks and for the final vanishing of the splitting for  $\log(z) = -1$  (Fig. 5C). When  $\log(z) > 2$ , the chemical reaction is very fast, its equilibrium is maintained all throughout the voltammetric experiment, thus the surface concentration of B is not affected by the chemical reaction during the time scale

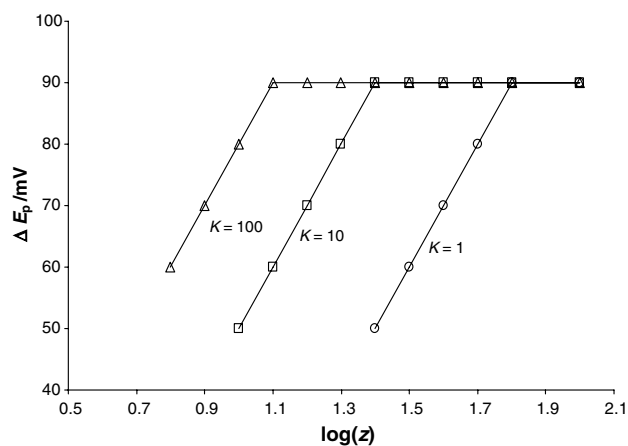


Fig. 6. Fast electron transfer: The effect of the chemical parameter  $z$  to the potential separation between the split SW peaks simulated for three values of equilibrium constant  $K$ .  $\lambda = 10$ , while the other conditions were the same as in Fig. 1.

of the experiment. Under such conditions, the behaviour of the system is equivalent to the simple surface electrode reaction, thus the splitting appears again (Fig. 5E). Such remarkable behaviour of the system, under the influence of the chemical kinetic parameter, can be used as a simple indicator for qualitative recognizing of the surface CE mechanism.

Shown in Fig. 6 is the dependence of potential separation between the split net SW peaks,  $\Delta E_p$ , on  $\log(z)$ , simulated for three values of  $K$ . The linear parts of the dependencies in Fig. 6 are associated with the following regression lines:

$$\Delta E_p/\text{mV} = 100 \log(z) - 90 \quad (\text{for } K = 1), \quad (9a)$$

$$\Delta E_p/\text{mV} = 100 \log(z) - 50 \quad (\text{for } K = 10), \quad (9b)$$

$$\Delta E_p/\text{mV} = 100 \log(z) - 20 \quad (\text{for } K = 100) \quad (9c)$$

that are valid for  $nE_{sw} = 50$  mV,  $dE = 10$  mV, and  $\alpha = 0.5$ . The Eqs. (9a)–(9c) can be explored for estimating of the value of the chemical parameter  $z$ , provided that the values of the standard rate constant  $k_s$  and the equilibrium constant  $K$  are known.

## 4. Conclusions

In the last two decades, square-wave voltammetry emerges as one of the leading voltammetric techniques in respect of the kinetics characterization of various electrode reactions. It offers relative simple modes for recognition of the electrode mechanisms, as well as for measuring of their kinetics. In this communication, the voltammetric features of a surface CE reaction have been theoretically studied under conditions of square-wave voltammetry. The major characteristics of this mechanism can be summarized as follows:

- The surface CE reactions with *slow electron transfer* are characterized by sigmoidal dependence of the dimensionless peak currents on the logarithm of the equilibrium constant of the preceding chemical reaction  $K$ , and on the logarithm of the chemical parameter  $\log(z)$ .
- The theoretical curves of the SW peak potentials of *slow electron transfer* surface CE reactions, as a function of  $\log(K)$  and  $\log(z)$ , have sigmoidal forms, too. In general, the increase of  $K$  is followed by shifting of the peak potentials in positive directions, while the increasing of the chemical parameter  $z$  leads to shifting of the SW peak potentials in negative direction.
- The *slow electron transfer* surface CE reactions have a feature of a “quasireversible maximum”. The position of the quasireversible maximum depends neither on  $z$  nor on  $K$ .
- The surface CE systems, characterized with *fast electron transfer* reaction, show the feature of split SW peaks. The shapes of the voltammetric responses in such case are function of the kinetics and thermodynamics of the preceding chemical reaction, as well as of the square-wave amplitude.

We show here that square-wave voltammetry provides a unique way for recognizing of the surface CE reaction, and offers simple manners for measuring the kinetics and thermodynamics of such systems. By exploring features of the *quasireversible maximum* (see Fig. 3), one can determine the *standard electron exchange rate constant*  $k_s$ . The *equilibrium constant*  $K$  of the preceding chemical reaction can be determined from the slope of the linear parts of the dependence of peak potentials  $E_p$  vs. the logarithm of the chemical parameter  $\log(z)$  (see Fig. 2B). Finally, knowing the values of  $k_s$  and  $K$ , the *splitting* of the net SW peak under large SW amplitude can be exploited for *estimation of the kinetics of the preceding chemical reaction* (see Fig. 6 and Eqs. (9a)–(9c)). Therefore, square-wave voltammetry enables complete kinetic and thermodynamic characterization of the surface CE electrode mechanism, without additional help of a secondary technique, like cyclic voltammetry or electrochemical impedance spectroscopy.

### Acknowledgements

Rubin Gulaboski thanks Fundação para a Ciência e a Tecnologia (FCT) of Portugal for providing of a post. doc. fellowship (SFRH/BPD/14894/2004). Valentin Mirčeski thanks Alexander von Humboldt Foundation and Ministry of Education and Science of Republic of Macedonia for financial support.

### References

- [1] D.E. Smith, Anal. Chem. 35 (1963) 602.
- [2] J. Osteryoung, J.J. O’Dea, in: Bard A.J. (Ed.), Electroanalytical Chemistry, A Series of Advances, vol 14, Marcel Dekker, New York, 1986, p. 228.
- [3] J.J. O’Dea, J.G. Osteryoung, Anal. Chem. 65 (1993) 3090.
- [4] J.J. O’Dea, K. Wikiel, J. Osteryoung, J. Phys. Chem. 94 (1990) 3628.
- [5] J. Osteryoung, R.A. Osteryoung, Anal. Chem. 57 (1985) 101A.
- [6] J.J. O’Dea, J. Osteryoung, R.A. Osteryoung, Anal. Chem. 53 (1981) 13.
- [7] J.J. O’Dea, J. Osteryoung, Anal. Chem. 65 (1993) 3090.
- [8] J.J. O’Dea, J. Osteryoung, Anal. Chem. 69 (1997) 650.
- [9] A. Webber, M. Shah, J. Osteryoung, Anal. Chim. Acta 157 (1984) 1.
- [10] A. Webber, J. Osteryoung, Anal. Chim. Acta 157 (1984) 17.
- [11] J.J. O’Dea, A. Ribes, J. Osteryoung, J. Electroanal. Chem. 345 (1993) 287.
- [12] J.J. O’Dea, J. Osteryoung, R.A. Osteryoung, J. Phys. Chem. 87 (1983) 3911.
- [13] V. Mirčeski, R. Gulaboski, Electroanalysis 13 (2001) 1326.
- [14] V. Mirčeski, R. Gulaboski, J. Solid, State Electrochem. 7 (2003) 157.
- [15] R. Bilewicz, R.A. Osteryoung, J. Osteryoung, Anal. Chem. 58 (1986) 261.
- [16] M.M. Correia dos Santos, M.L. Simoes Goncalves, J.C. Romao, J. Electroanal. Chem. 413 (1996) 97.
- [17] F. Garay, M. Lovrić, J. Electroanal. Chem. 518 (2002) 91.
- [18] A.B. Miles, R.G. Compton, J. Electroanal. Chem. 499 (2001) 1.
- [19] A.B. Miles, R.G. Compton, J. Electroanal. Chem. 487 (2000) 75.
- [20] A.B. Miles, R.G. Compton, J. Phys. Chem. B 104 (2000) 5331.
- [21] T.M. Saccucci, J.F. Rusling, J. Phys. Chem. B 105 (2001) 6142.
- [22] M. Rudolph, J. Electroanal. Chem. 503 (2001) 15.
- [23] A. Molina, C. Serna, F. Martinez-Ortiz, J. Electroanal. Chem. 486 (2000) 9.
- [24] E. Laviron, J. Electroanal. Chem. 42 (1973) 415.
- [25] E. Laviron, J. Electroanal. Chem. 101 (1979) 19.
- [26] R. Meunier-Prest, E. Laviron, J. Electroanal. Chem. 410 (1996) 133.
- [27] M. Penczek, Z. Stojek, J. Buffle, J. Electroanal. Chem. 270 (1989) 1.
- [28] M. Lovrić, Š. Komorsky-Lovrić, R. Murray, Electrochim. Acta 33 (1988) 739.
- [29] M. Lovrić, Š. Komorsky-Lovrić, J. Electroanal. Chem. 384 (1995) 115.
- [30] Š. Komorsky-Lovrić, M. Lovrić, Electroanalysis 8 (1996) 959.
- [31] V. Mirčeski, R. Gulaboski, Croat. Chim. Acta 75 (2003) 37.
- [32] V. Mirčeski, R. Gulaboski, Microchim. Acta 138 (2002) 33.
- [33] V. Mirčeski, M. Lovrić, R. Gulaboski, J. Electroanal. Chem. 515 (2001) 91.
- [34] V. Mirčeski, M. Lovrić, Electroanalysis 9 (1997) 1283.
- [35] M. Lovrić, Š. Komorsky-Lovrić, J. Electroanal. Chem. 248 (1988) 239.
- [36] (a) Y.I. Turyan, J. Electroanal. Chem. 338 (1992) 1;  
(b) Y.I. Turyan, M. Lovrić, J. Electroanal. Chem. 531 (2002) 147.
- [37] F.A. Armstrong, H.A. Heering, J. Hirst, Chem. Soc. Rev. 26 (1997) 169.
- [38] J. Hirst, G.N.L. Jameson, J.W.A. Allen, F.A. Armstrong, J. Am. Chem. Soc. 120 (1998) 11994.
- [39] F.A. Armstrong, G.S. Wilson, Electrochim. Acta 45 (2000) 2623.
- [40] J. Hirst, F.A. Armstrong, Anal. Chem. 70 (1998) 5062.
- [41] R.S. Nicholson, M.L. Olmstead, in: J.S. Mattson, H.B. Mark, H.C. MacDonald (Eds.), Electrochemistry: Calculations, Simulation and Instrumentation, vol. 2, Marcel Dekker, New York, 1972, pp. 120–137.